SUPPLEMENTARY INFORMATION

Selective In Vivo Metabolic Cell Labeling Mediated Cancer Targeting

Hua Wang[b,*], Ruibo Wang[b,*], Kaimin Cai[b,*], Hua He[a], Yang Liu[b], Jonathan Yen[c], Zhiyu Wang[b], Ming Xu[b], Yiwen Sun[b], Xin Zhou[d], Qian Yin[b], Li Tang[b], Iwona T. Dobrucki[e], Lawrence W. Dobrucki[c], Eric J. Chaney[f], Stephen A. Boppart[c,f,g,h], Timothy M. Fan[i,1], Stéphane Lezmi[j,1], Xuesi Chen,[p,1] Lichen Yin[a,1], Jianjun Cheng[a,b,c,k,l,m,n,o,1]

[a]Jiangsu Key Laboratory for Carbon-Based Functional Materials & Devices, Institute of Functional Nano & Soft Materials (FUNSOM), Soochow University, Suzhou 215123, Jiangsu, China.
[b]Department of Materials Science and Engineering, [c]Department of Bioengineering, [e]Molecular Imaging Laboratory, Beckman Institute for Advanced Science and Technology, [f]Biophotonics Imaging Laboratory, Beckman Institute for Advanced Science and Technology, [g]Department of Electrical and Computer Engineering, [h]Department of Internal Medicine, [i]Department of Veterinary Clinical Medicine, [j]Department of Pathobiology at College of Veterinary Medicine, [k]Department of Chemistry, [l]Beckman Institute for Advanced Science and Technology, [m]Micro and Nanotechnology Laboratory, [n]Institute of Genomic Biology, [o]Materials Research Laboratory, University of Illinois at Urbana–Champaign, Urbana, IL, 61801, USA.
[d]Department of Chemistry, University of Science and Technology of China, Hefei, Anhui 230026, China.
[p]Key Laboratory of Polymer Ecomaterials, Changchun Institute of Applied Chemistry, Changchun 130022, People's Republic of China

*These authors contributed equally to this work.

[1]To whom correspondence may be addressed. Email: jianjunc@illinois.edu; lcyin@suda.edu.cn; xschen@ciac.ac.cn; slezmi@illinois.edu; t-fan@illinois.edu.

Nature Chemical Biology: doi:10.1038/nchembio.2297

SUPPLEMENTARY RESULTS

SUPPLEMENTARY FIGURES

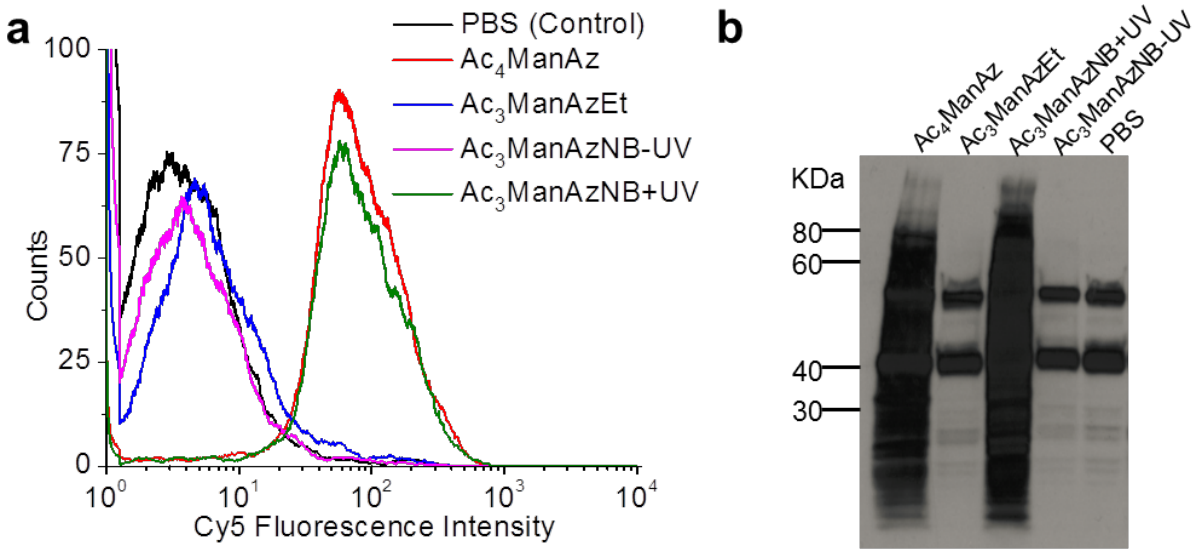

Supplementary Figure 1. Replacing the C1-OAc of Ac_4ManAz with a cleavable ether bond enabled controlled metabolic cell labeling in vitro. (a) Flow cytometry analysis of LS174T cells after treated with PBS, Ac_4ManAz, Ac_3ManAzEt, Ac_3ManAzNB-UV, and Ac_3ManAzNB+UV, respectively, for 72 h and labeled with DBCO-Cy5 for 1 h. UV irradiation with an intensity of 10 mW/cm^2 was applied for 10 min at the start of incubation. (b) Western blotting analysis of LS174T cells after treatment with Ac_4ManAz, Ac_3ManAzEt, Ac_3ManAzNB+UV, Ac_3ManAzNB-UV, and PBS, respectively, for 72 h. Azido-modified proteins were biotinylated by incubating with phosphine-PEG_4-biotin and then detected by streptavidin-horseradish peroxidase conjugate. Ac_3ManAzEt, Ac_3ManAzNB and PBS groups showed only two endogenous biotinylated protein bands.

Nature Chemical Biology: doi:10.1038/nchembio.2297

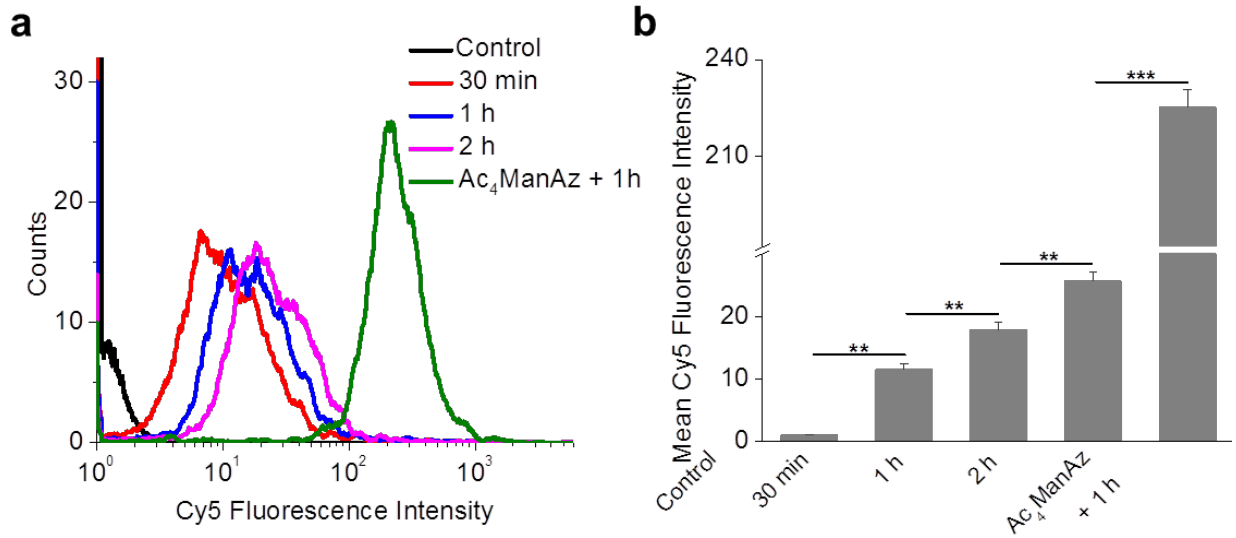

Supplementary Figure 2. **Comparison of active and passive uptake of DBCO-Cy5**. (a) Flow cytometry analyses of LS174T cells after incubation with DBCO-Cy5 for 30 min, 1 h, and 2 h, respectively. Cells without DBCO-Cy5 treatment were used as negative controls. Cells pretreated with Ac_4ManAz (50 μM) for three days and further treated with DBCO-Cy5 for 1 h were used for comparison. (b) Mean fluorescence intensity of LS174T cells for different groups in (a). Data were presented as mean ± SEM (n=6) and analyzed by one-way ANOVA (Fisher; $0.01 < *P \leq 0.05$; $**P \leq 0.01$; $***P \leq 0.001$).

Nature Chemical Biology: doi:10.1038/nchembio.2297

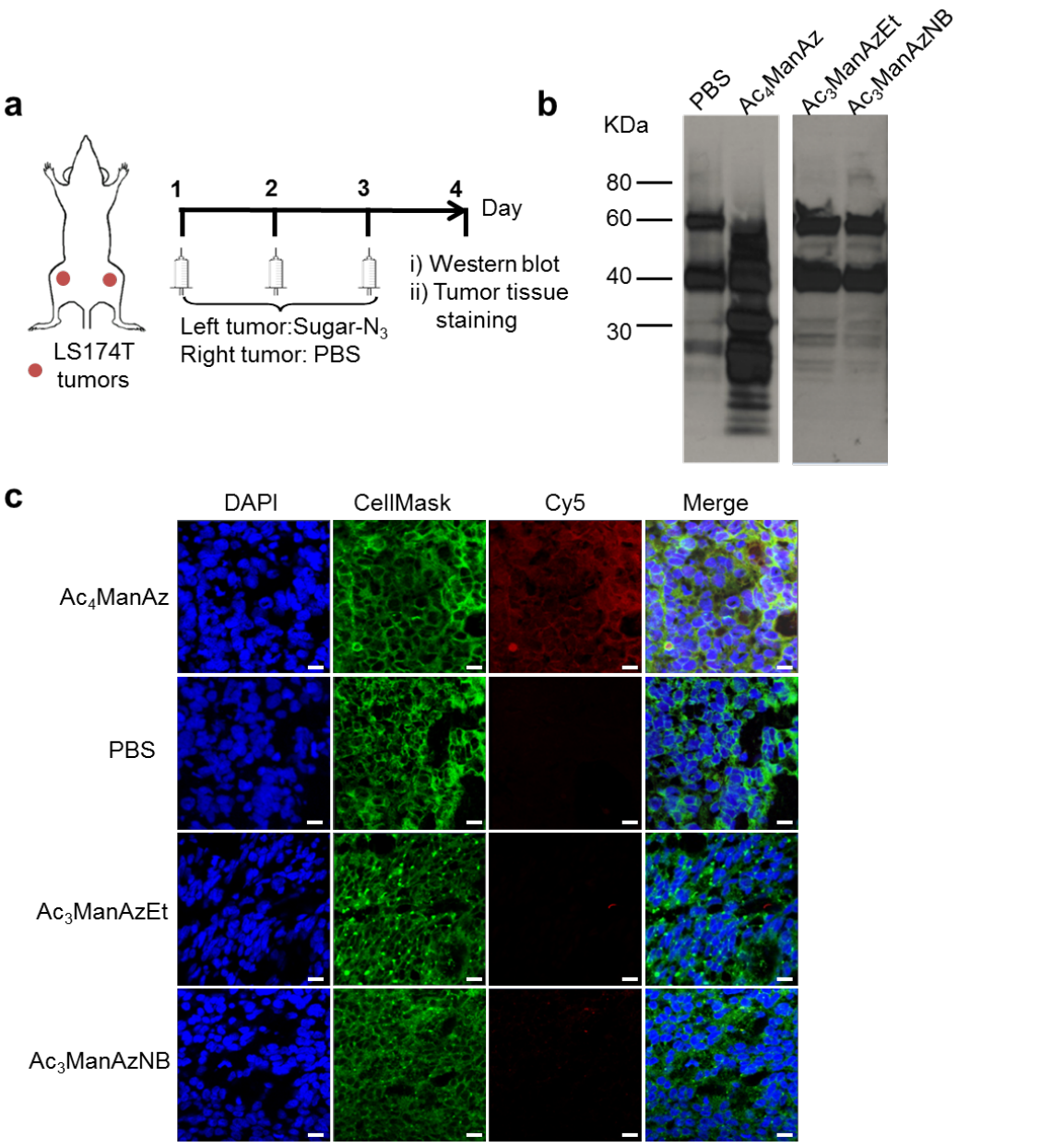

Supplementary Figure 3. **Ac_3ManAzEt and Ac_3ManAzNB showed blocked metabolic labeling activity in vivo**. (a) Time course of in vivo labeling study in athymic nude mice bearing subcutaneous LS174T tumors. When the tumors reached ~50 mm^3, Ac_4ManAz or Ac_3ManAzEt or Ac_3ManAzNB (25 mM, 20 μL) was injected to the left tumors once daily for three days. The right tumors were injected with PBS as controls. (b) Western blotting analysis of tumor tissues treated with PBS, Ac_4ManAz, Ac_3ManAzEt, and Ac_3ManAzNB, respectively. Azido-modified proteins were first biotinylated by incubating with phosphine-PEG_4-biotin, and then detected by streptavidin-horseradish peroxidase conjugate. (c) CLSM images of tumor tissue sections from different groups. Tumor tissues were blocked with BSA for 2 h and then labeled with DBCO-Cy5 (red) for 30 min. Cell nuclei and membrane were stained with DAPI (blue) and CellMask orange plasma membrane stain (green), respectively. Scale bar: 10 μm.

Nature Chemical Biology: doi:10.1038/nchembio.2297

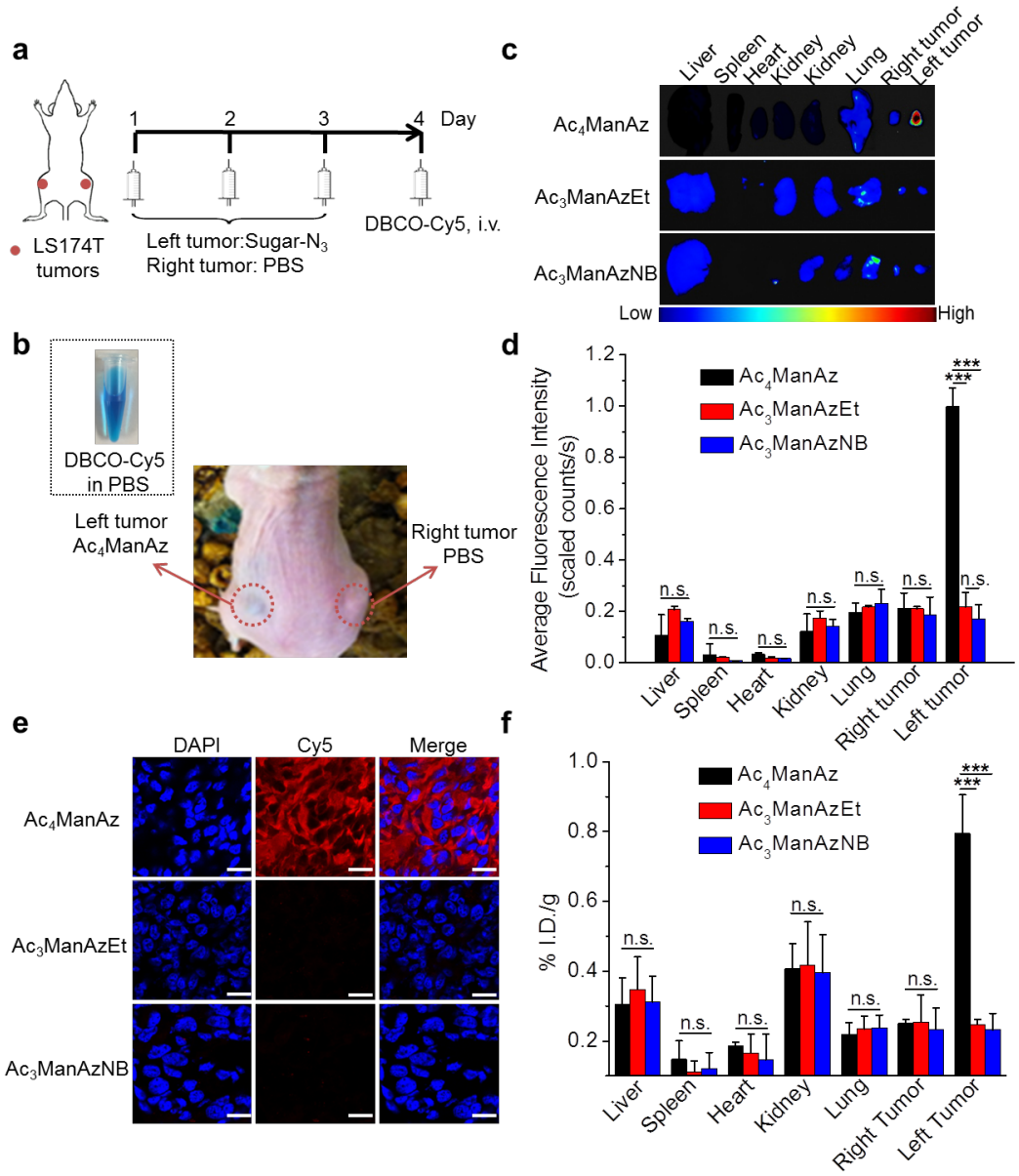

Supplementary Figure 4. **Tumor accumulation of DBCO-Cy5 was significantly improved in azido-modified tumors**. (a) Time course of in vivo labeling study in athymic nude mice bearing subcutaneous LS174T tumors. Sugar-N_3 (25 mM, 20 μL) was injected to the left tumors once daily for three days (Day 1-3), and the right tumors were injected with PBS as controls. DBCO-Cy5 (5 mg/kg) was i.v. injected on Day 4, and mice were sacrificed for analysis at 48 h p.i. of DBCO-Cy5. (b) Picture of mouse at 48 h p.i. of DBCO-Cy5. The left tumor injected with Ac_4ManAz showed the intrinsic blue color of DBCO-Cy5, and the right tumor injected with PBS showed no blue color. A picture of DBCO-Cy5 solution was shown. (c) Fluorescence imaging of harvested tissues from different group mice. (d) Fluorescence intensity of tissues (n=3) from (c). (e) CLSM images of tumor tissue sections from different groups. The cell nuclei were stained with DAPI (blue). Scale bar: 20 μm. (f) Retained Cy5 in tissues from different groups (n=3). All of the numerical data were presented as mean ± SEM and analyzed by one-way ANOVA (Fisher; $0.01 < *P \leq 0.05$; $**P \leq 0.01$; $***P \leq 0.001$).

Nature Chemical Biology: doi:10.1038/nchembio.2297

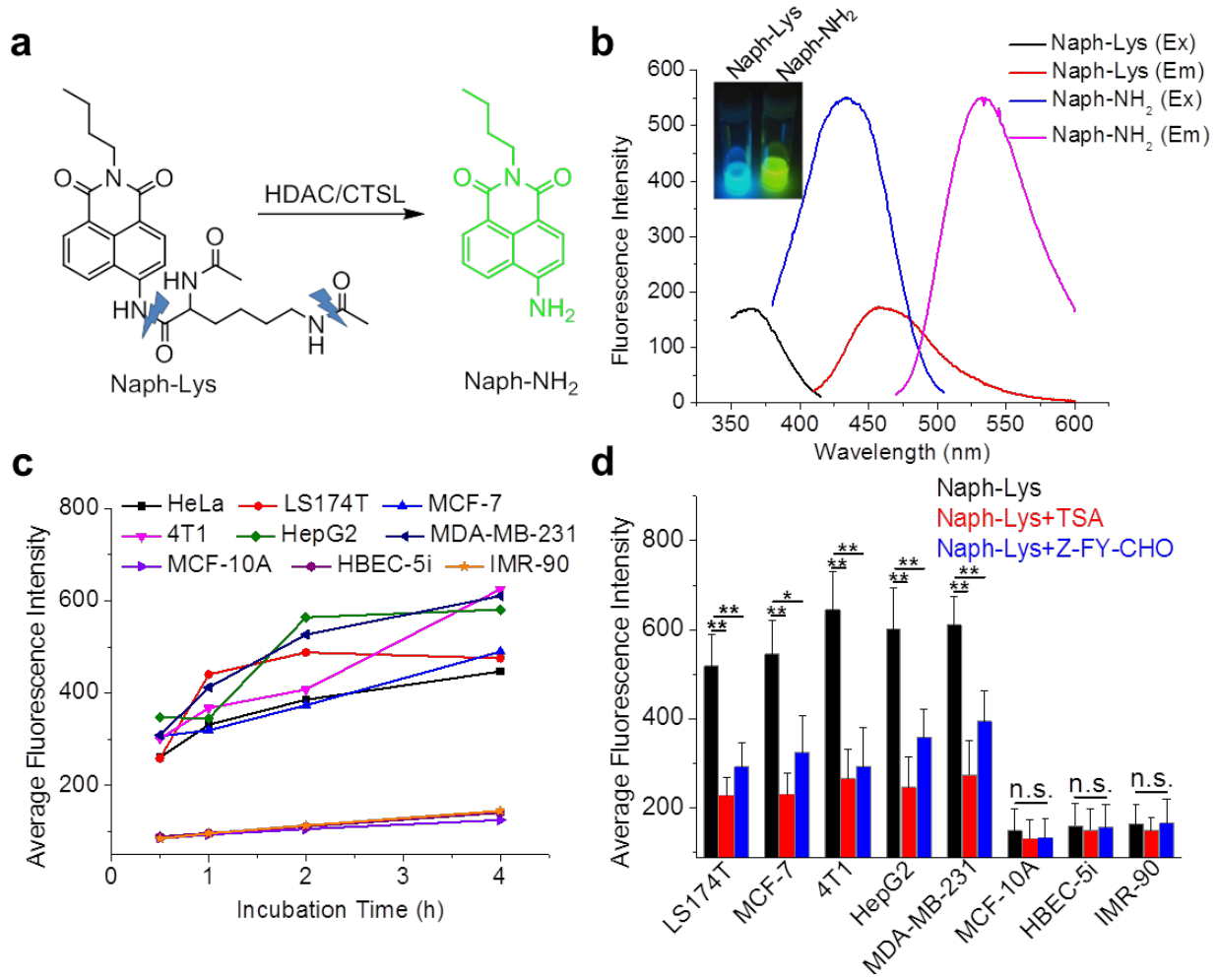

Supplementary Figure 5. **HDAC and CTSL are overexpressed in various cancer cell lines**. (a) Structure of the HDAC/CTSL fluorescence turn-on reporter (Naph-Lys) and its degradation product (Naph-NH_2) in the presence of HDAC/CTSL. (b) Excitation and emission spectra of Naph-Lys (5 μg/mL in methanol) and Naph-NH_2 (200 ng/mL in methanol). (c) Detection of HDAC/CTSL activity in different cell lines (HeLa, black; LS174T, red; MCF-7, blue; 4T1, magenta; HepG2, olive; MDA-MB-231, navy; MCF-10A, violet; HBEC-5i, purple; IMR-90, orange). (d) Average fluorescence intensity of different cell lines treated with Naph-Lys (50 μM), Naph-Lys (50 μM) + TSA (1 μM), and Naph-Lys (50 μM) + Z-FY-CHO (50 μM), respectively, for 4 h. Data were presented as mean ± SEM (n=6) and analyzed by one-way ANOVA (Fisher; $0.01 < *P \leq 0.05$; $**P \leq 0.01$; $***P \leq 0.001$).

Nature Chemical Biology: doi:10.1038/nchembio.2297

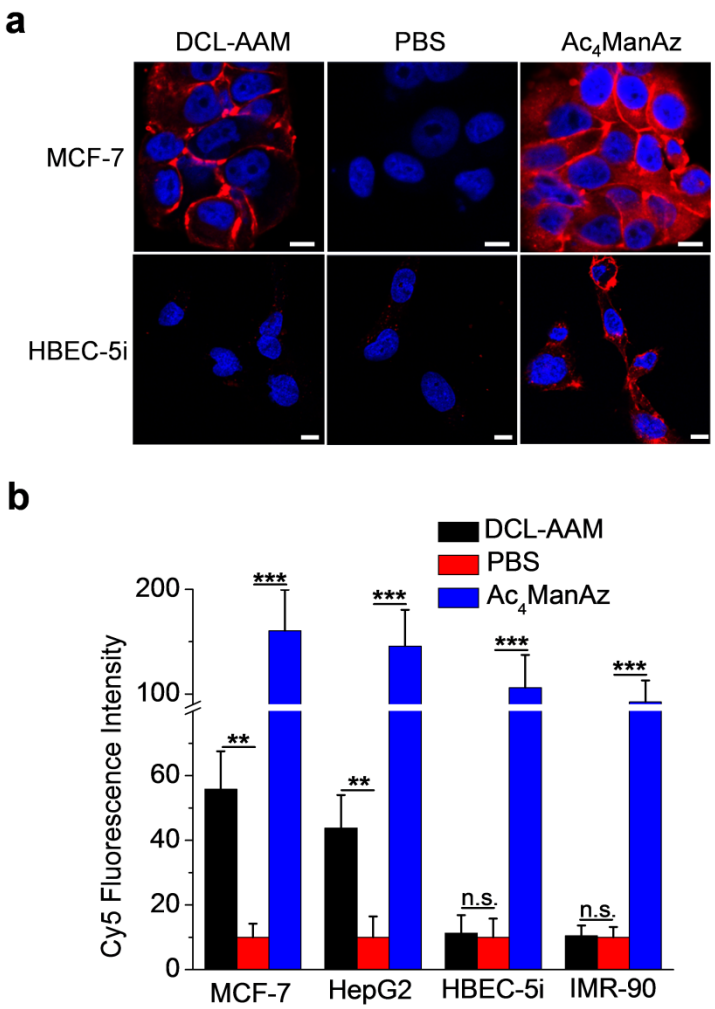

Supplementary Figure 6. **DCL-AAM mediated cancer-selective labeling in vitro**. (a) CLSM images of MCF-7 breast cancer cells (upper row) and HBEC-5i cerebral microvascular endothelium cells (lower row) after incubated with DCL-AAM (50 μM) or PBS or Ac_4ManAz (50 μM) for 72 h and labeled with DBCO-Cy5 (50 μM) for 1 h. The cell nuclei were stained with DAPI (blue). Scale bar: 10 μm. (b) Average Cy5 fluorescence intensity of different cell lines (MCF-7, HepG2, HBEC-5i, and IMR-90 cells) following the same treatment as described in (a). Data were presented as mean ± SEM (n=6) and analyzed by one-way ANOVA (Fisher; 0.01 < $*P \leq 0.05$; $**P \leq 0.01$; $***P \leq 0.001$).

Nature Chemical Biology: doi:10.1038/nchembio.2297

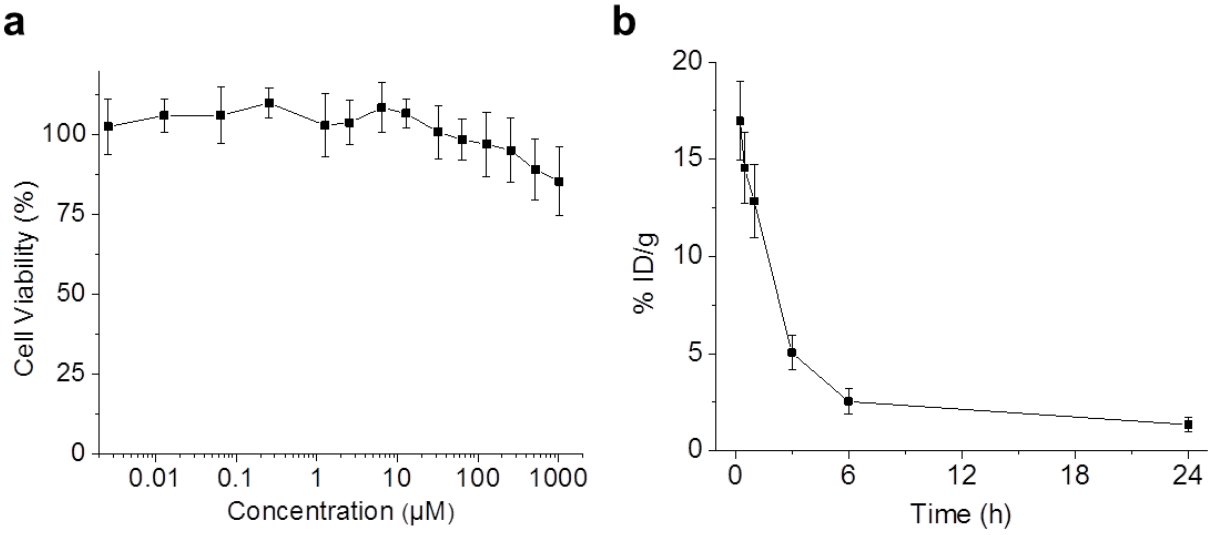

Supplementary Figure 7. **DCL-AAM showed minimum cytotoxicity and short circulation half-life**. (a) Cell Viability of LS174T cells after treated with different concentrations of DCL-AAM for 72 h, as determined by MTT assay. (c) Pharmacokinetic profile of ^{64}Cu-labeled E-S in athymic nude mice.

Nature Chemical Biology: doi:10.1038/nchembio.2297

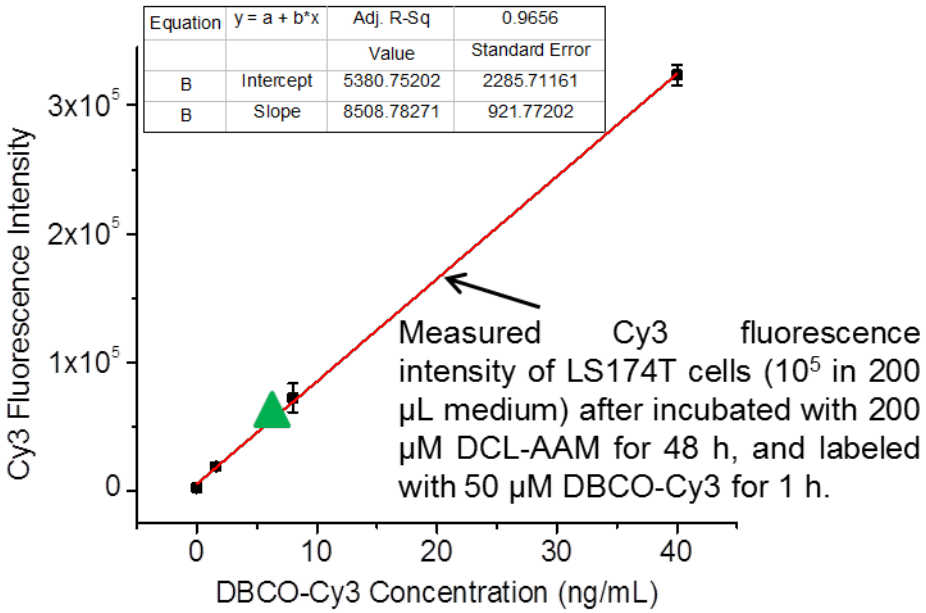

Mass of DBCO-Cy3 per cell: (7.5 ng/mL * 200 µ L)/100000 cells = $1.5 * 10^{-5}$ ng/cell
Moles of azides per cell: ($1.5 * 10^{-5}$ ng/cell)/(983.18 g/mol) = $1.5 * 10^{-17}$ mol
Number of azides per cell: $1.5* 10^{-17}$ moles * ($6.02 * 10^{23}$ mol^{-1}) = $9.0 * 10^{6}$

Supplementary Figure 8. Estimation of number density of azido groups on the surface of LS174T cells after incubated with 200 µM DCL-AAM for 48 h and labeled with 50 µM DBCO-Cy3 for 1 h.

Nature Chemical Biology: doi:10.1038/nchembio.2297

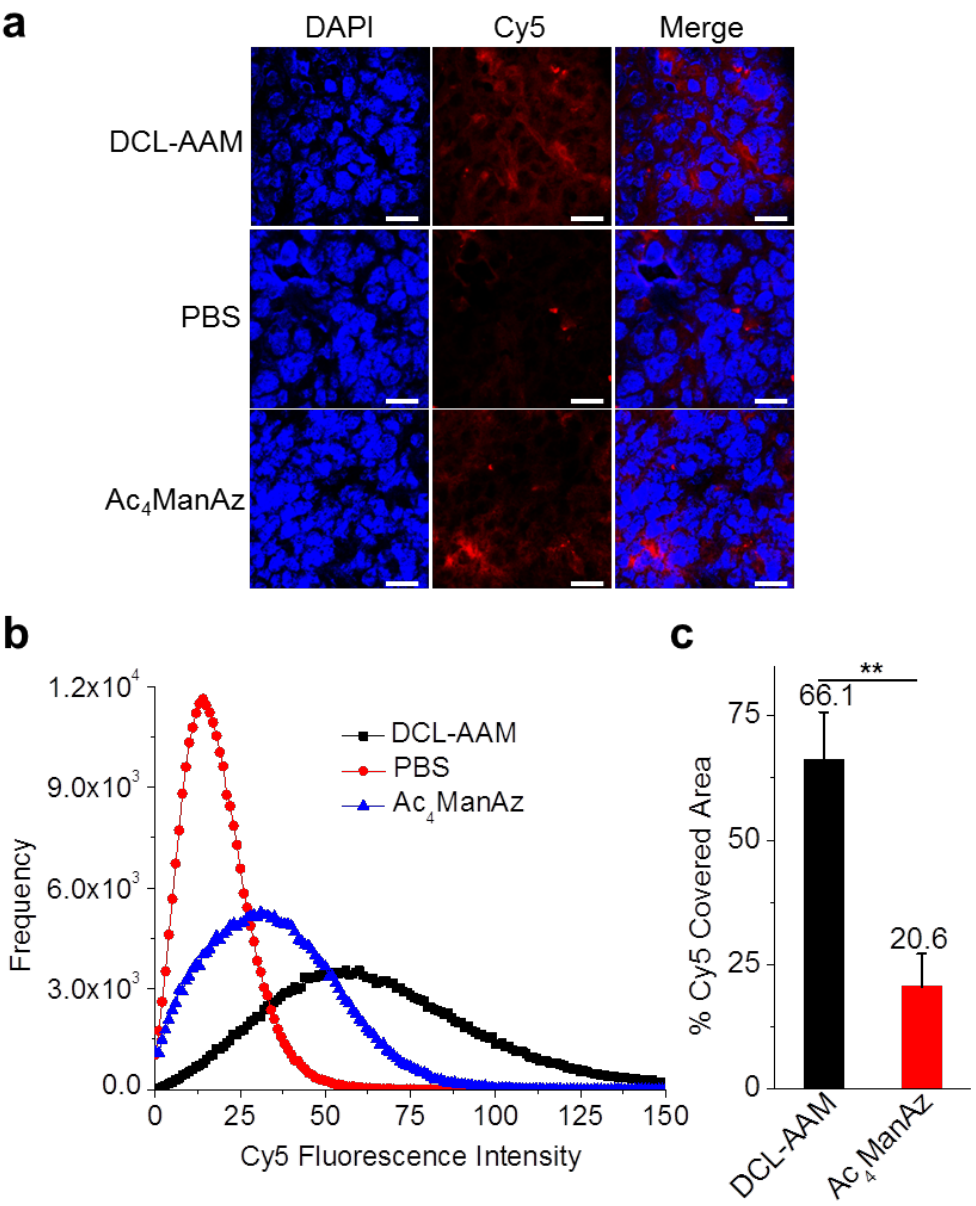

Supplementary Figure 9. **DCL-AAM showed superior in vivo cancer-selective labeling capability in comparison with Ac_4ManAz**. DCL-AAM (60 mg/kg), Ac_4ManAz (40 mg/kg) or PBS was i.v. injected into athymic nude mice bearing subcutaneous LS174T tumors once daily for three days. DBCO-Cy5 (10 mg/kg) was i.v. injected at 24 h post the last injection of azido-sugars. Mice were sacrificed at 48 h p.i. of DBCO-Cy5. (a) CLSM images of tumor sections from mice treated with DCL-AAM, Ac_4ManAz, and PBS, respectively. The cell nuclei were stained with DAPI (blue). Scale bar: 20 μm. (b) Cy5 fluorescence intensity profiles of tumor sections extracted from (a) and averaged over 20 images. (c) Percentage of Cy5-covered area of tumor tissue sections which was calculated from (b) and defined as: the sum of frequency (Cy5 fluorescence intensity ≥ 50 a.u.) divided by the total frequency.

Nature Chemical Biology: doi:10.1038/nchembio.2297

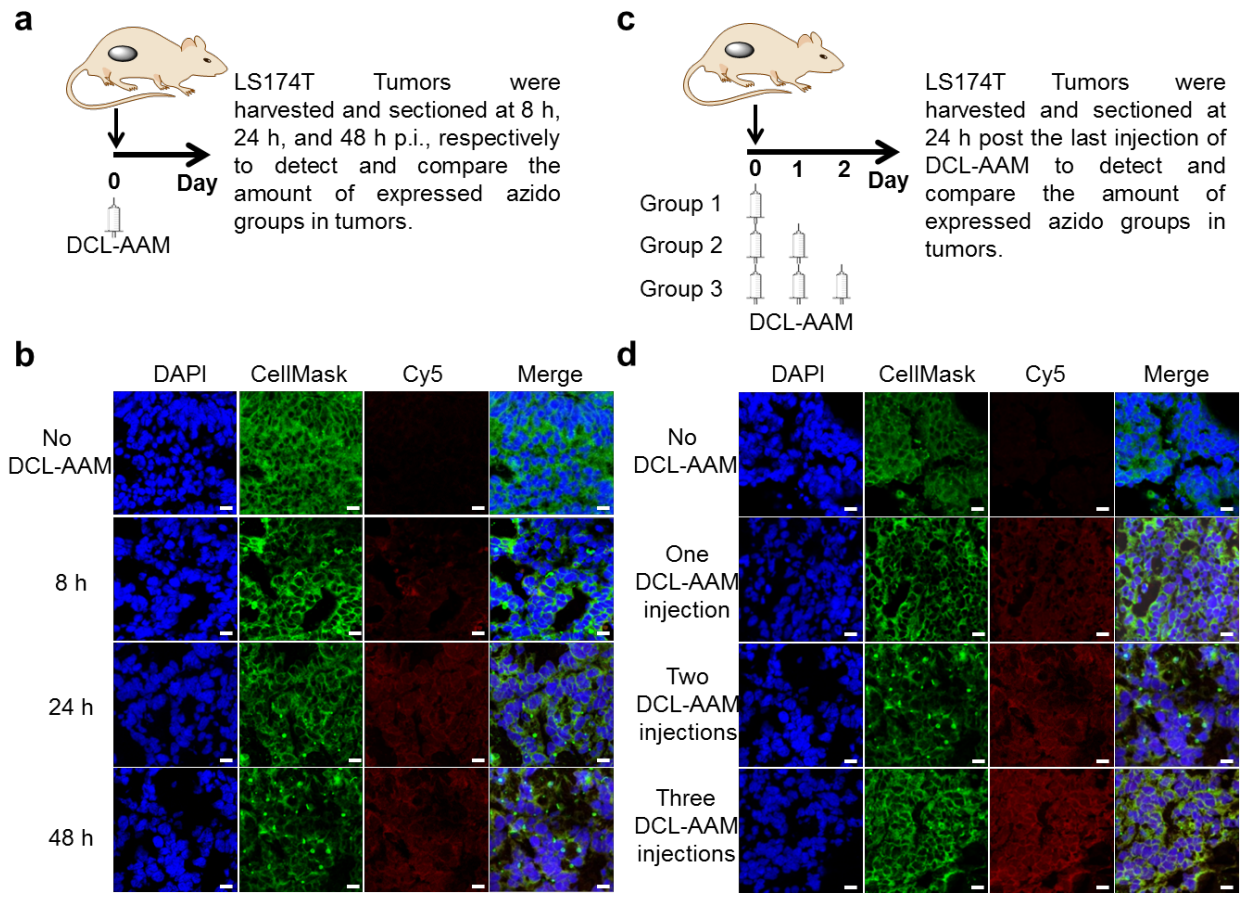

Supplementary Figure 10. DCL-AAM mediated tumor labeling in vivo was time- and dose frequency-dependent. (a-b): In vivo tumor labeling kinetics of DCL-AAM. (a) Time course of in vivo labeling kinetics study. Athymic nude mice bearing subcutaneous LS174T tumors were i.v. injected with DCL-AAM (60 mg/kg). Tumors were harvested and sectioned at 8, 24, and 48 h p.i. of DCL-AAM, respectively, for determining the time-course expression profiles of azido groups. (b) CLSM images of tumor tissue sections harvested at 8, 24, and 48 h p.i. of DCL-AAM (60 mg/kg), respectively. Tumor tissue sections were blocked with 5% BSA for 2 h and then labeled with DBCO-Cy5 (red) for 30 min. Cell nuclei and membrane were stained with DAPI (blue) and CellMask orange plasma membrane stain (green), respectively. Scale bar: 10 μm. (c-d): Dose frequency-dependent DCL-AAM mediated tumor labeling in vivo. (c) Time course of in vivo labeling study. Athymic nude mice bearing subcutaneous LS174T tumors were i.v. administered with DCL-AAM (60 mg/kg) for once, twice, and three times, respectively. Tumors were harvested and sectioned at 24 h post the last injection of DCL-AAM. (d) CLSM images of tumor tissue sections harvested from athymic nude mice with 0, 1, 2, and 3 injections of DCL-AAM, respectively, following the same treatment as described in (b). Scale bar: 10 μm.

Nature Chemical Biology: doi:10.1038/nchembio.2297

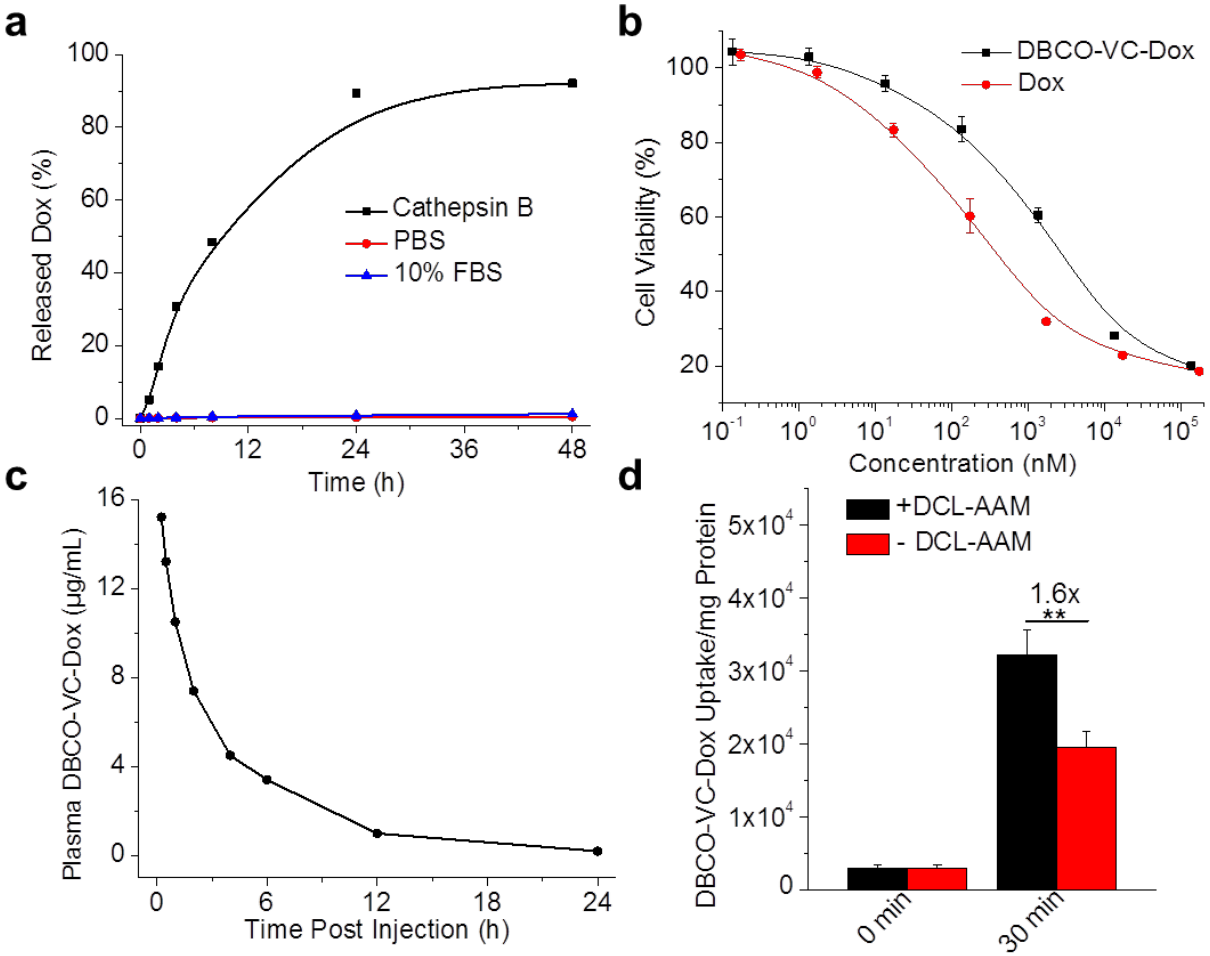

Supplementary Figure 11. **Characterizations of DBCO-VC-Dox**. (a) Release profile of DBCO-VC-Dox in the presence of activated cathepsin B, PBS, and 10% FBS, respectively. (b) Viability of LS174T cells after treated with DBCO-VC-Dox or Dox at various concentrations for 72 h. The data were presented as mean ± SEM, n = 6. (c) Pharmacokinetic profiles of DBCO-VC-Dox in athymic nude mice. (d) DBCO-VC-Dox uptake by LS174T cells with or without DCL-AAM pretreatment (72 h) over 30-min incubation. Cells without DBCO-VC-Dox treatment (0 min) were used as negative controls. Data were presented as mean ± SEM (n=6) and analyzed by one-way ANOVA (Fisher; $0.01 < *P \leq 0.05$; $**P \leq 0.01$; $***P \leq 0.001$).

Nature Chemical Biology: doi:10.1038/nchembio.2297

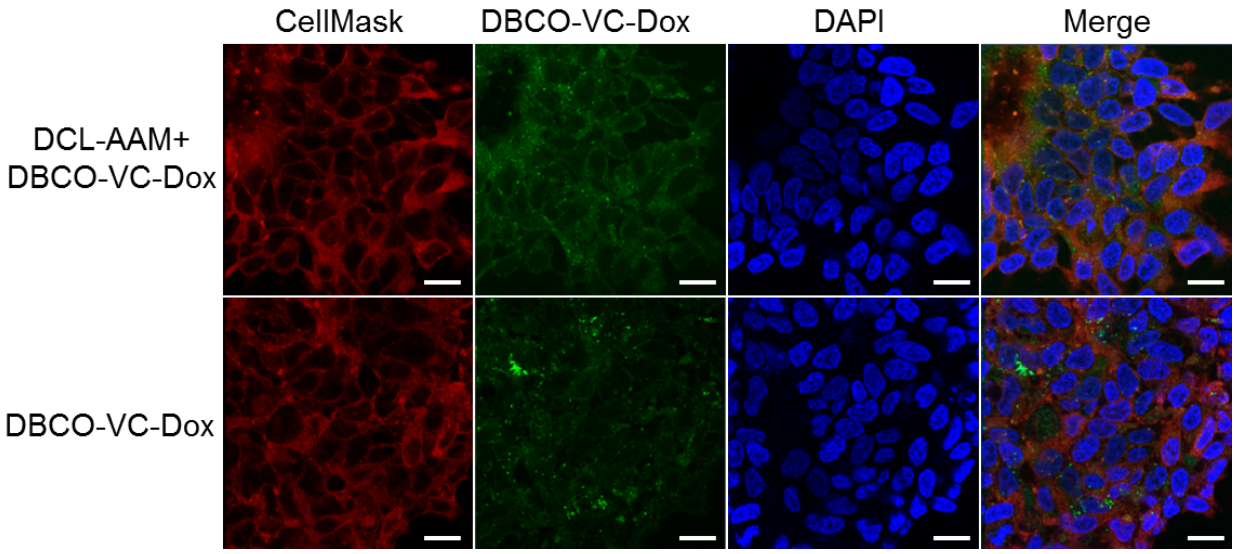

Supplementary Figure 12. **DBCO-VC-Dox was partially covalently attached to DCL-AAM treated LS174T cells**. LS174T cells were pretreated with DCL-AAM (50 μM) or PBS for three days, labeled with DBCO-VC-Dox (20 μM) for 1 h, and imaged under a confocal microscope. Cell membrane and nuclei were stained with CellMask deep red plasma membrane stain (red) and DAPI (blue), respectively. Scale bar: 10 μm.

Nature Chemical Biology: doi:10.1038/nchembio.2297

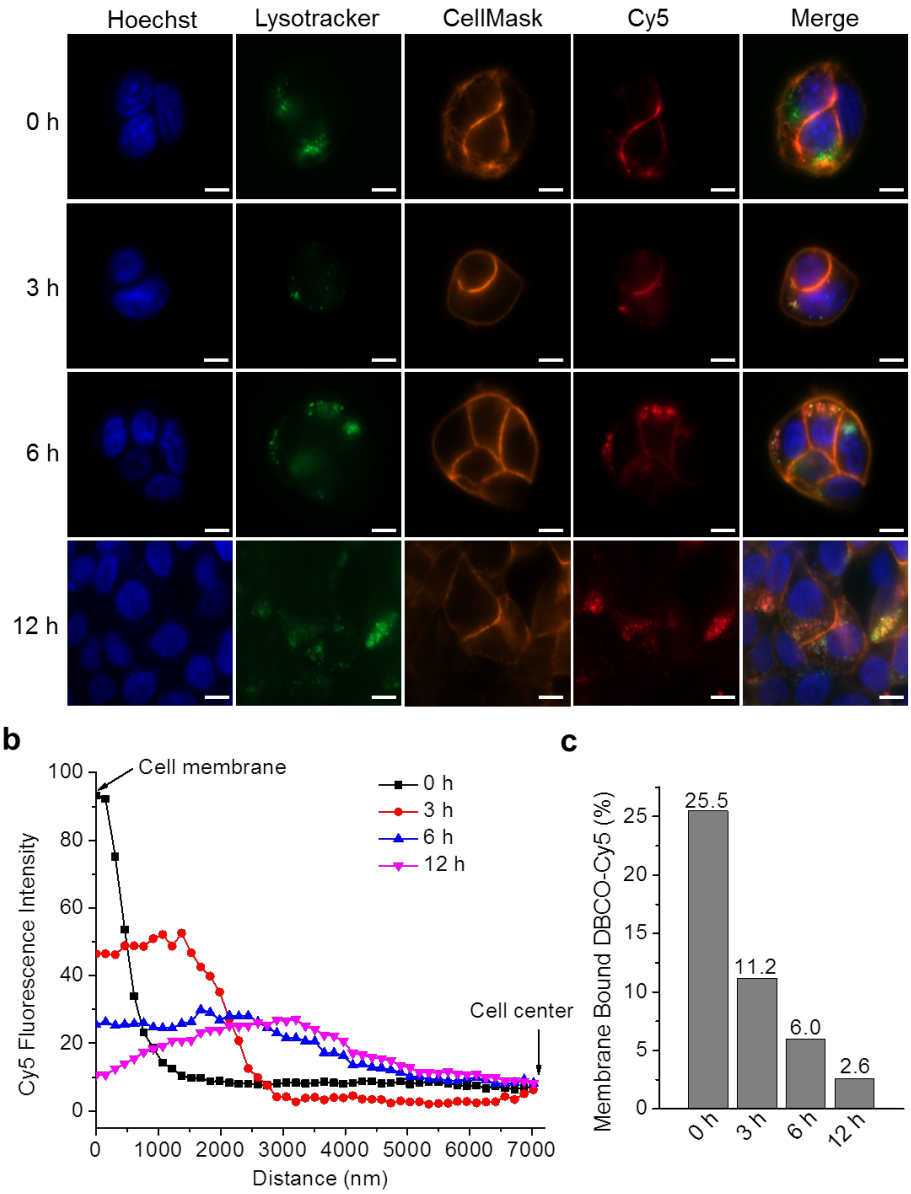

Supplementary Figure 13. Covalently attached DBCO-Cy5 entered endosomes/lysosomes in DCL-AAM treated LS174T cells. LS174T cells were pretreated with DCL-AAM (50 μM) for three days and labeled with DBCO-Cy5 (50 μM) for 1 h. After washing with PBS, cells were further incubated in fresh medium for different time (0, 3, 6, and 12 h) and imaged under a fluorescence microscope. (a) CLSM images of LS174T cells that were further incubated for 0, 3, 6, and 12 h, respectively. Endosomes/lysosomes were stained with Lysotracker green (green). Cell membrane and nuclei were stained with CellMask orange plasma membrane stain (orange) and Hoechst 33342 (blue), respectively. Scale bar: 10 μm. (b) Cy5 fluorescence intensity profile over the longitudinal direction of cells from (a). For each cell, the Cy5 fluorescence intensity profile over the longitudinal direction was extracted from CLSM image using ZEN software, with the longitudinal diameter of cell normalized to 14.5 μm. The profiles were then averaged over 30 cells for each group. (c) Percentage of membrane-bound DBCO-Cy5 for different further-incubation time, as calculated from (b) and defined as the sum of Cy5 fluorescence counts of 100-7000 nm interval divided by the total fluorescence counts of 0-7000 nm.

Nature Chemical Biology: doi:10.1038/nchembio.2297

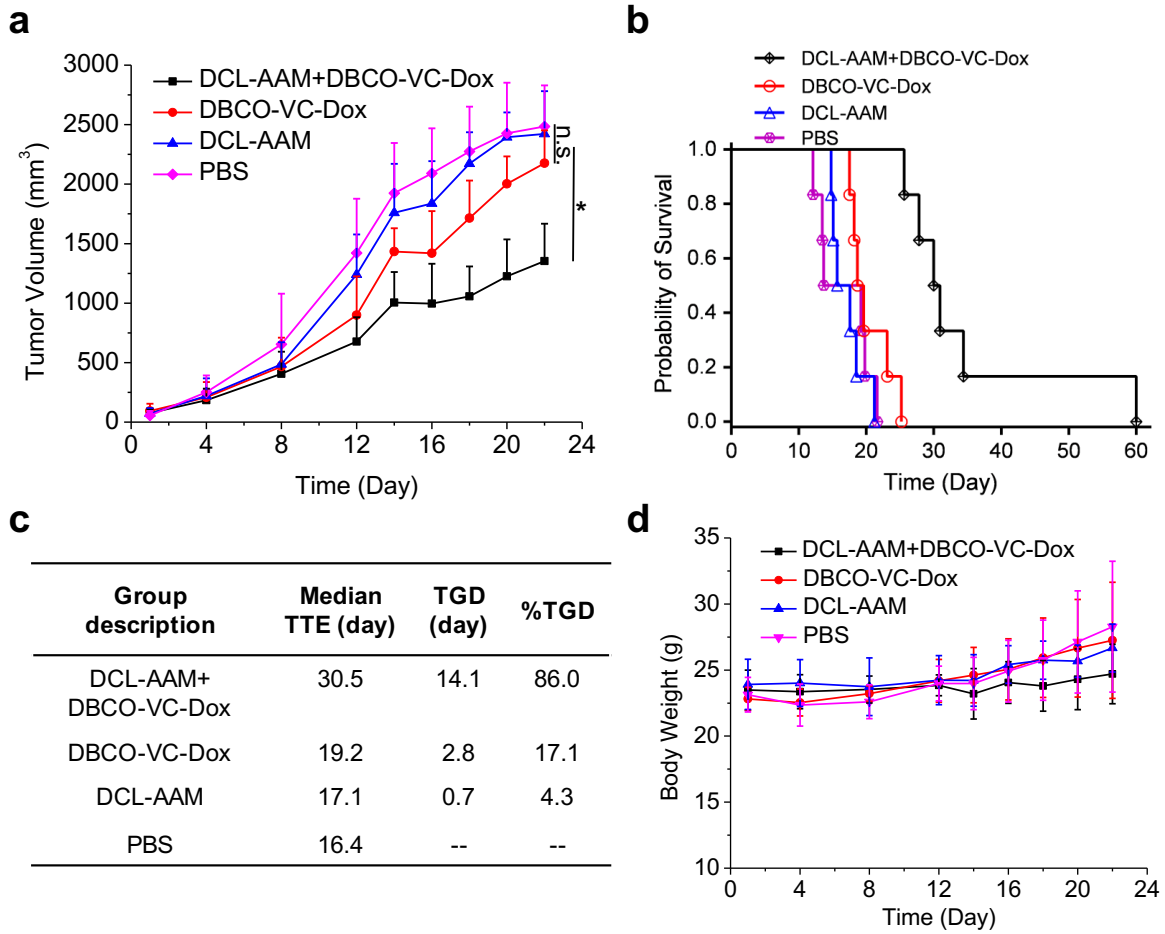

c

Group description	Median TTE (day)	TGD (day)	%TGD
DCL-AAM+ DBCO-VC-Dox	30.5	14.1	86.0
DBCO-VC-Dox	19.2	2.8	17.1
DCL-AAM	17.1	0.7	4.3
PBS	16.4	--	--

Supplementary Figure 14. **DCL-AAM mediated tumor labeling significantly improved long-term antitumor efficacy of DBCO-VC-Dox against subcutaneous LS174T tumors in athymic nude mice**. LS174T tumors were established in 6 week-old female athymic nude mice by subcutaneous injection of LS174T cells into both flanks. When the tumors reached ~50 mm^3, mice were randomly divided into 4 groups (group 1: DCL-AAM+DBCO-VC-Dox; group 2: DBCO-VC-Dox; group 3: DCL-AAM; group 4: PBS; n = 5-6). DCL-AAM (60 mg/kg) was i.v. injected on Day 0, 1, and 2. DBCO-VC-Dox (12 mg/kg) in Dox equivalent) was i.v. injected on Day 3, 7, and 11. Tumor volume and body weight were measured every other day. (a) Average LS174T tumor volume of mice from different groups over the course of the efficacy study. Data were presented as mean ± SEM (n=10) and analyzed by one-way ANOVA (Fisher; $0.01 < *P \leq 0.05$; $**P \leq 0.01$; $***P \leq 0.001$). (b) Kaplan-Meier plots for all groups. Loss of mice was because of treatment-related death or euthanasia after the predetermined end point was reached. (c) Survival analysis of mice from different groups. TTE: time to end point. TGD: tumor growth delay; TGD = TTE (treated group)－TTE (PBS group). %TGD = 100% × TGD/TTE (PBS group). (d) Body weight of mice from different groups over the course of the efficacy study.

Nature Chemical Biology: doi:10.1038/nchembio.2297

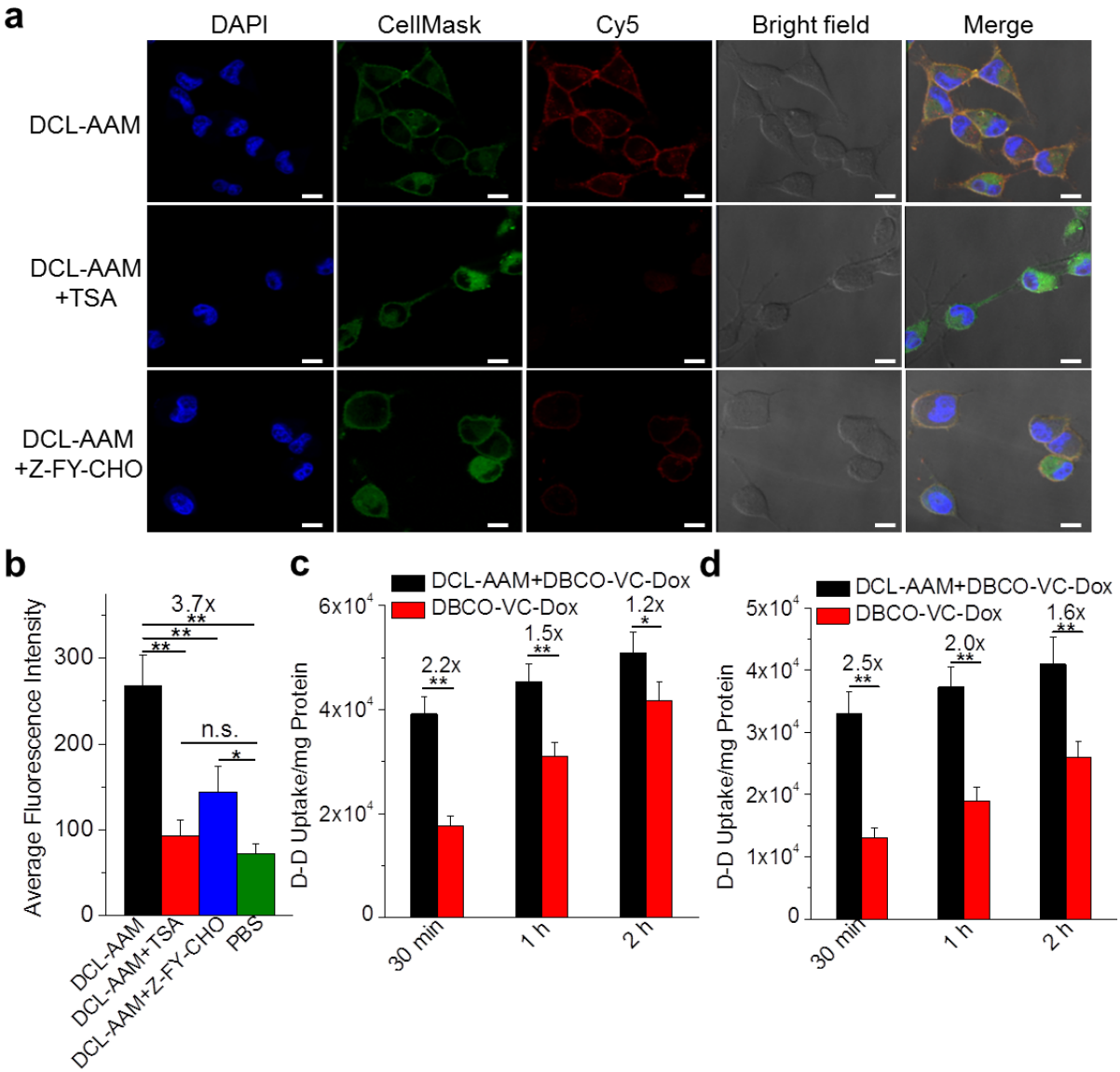

Supplementary Figure 15. **DCL-AAM could efficiently label MDA-MB-231 and 4T1 cells and resulted in enhanced uptake of DBCO-VC-Dox in vitro**. (a) CLSM images of MDA-MB-231 cells after incubated with DCL-AAM (50 μM), DCL-AAM (50 μM) + TSA (1 μM), and DCL-AAM (50 μM) + Z-FY-CHO (50 μM), respectively, for 72 h and labeled with DBCO-Cy5 (50 μM) for 1 h. The cell nuclei and membrane were stained with DAPI (blue) and CellMask orange plasma membrane stain (green), respectively. Scale bar: 10 μm. (b) Average Cy5 fluorescence intensity of MDA-MB-231 cells following the same treatment in (a). DBCO-VC-Dox uptake by MDA-MB-231 cells (c) and 4T1 cells (d) with or without DCL-AAM pretreatment (72 h) over different incubation time (30 min, 1 h, and 2 h). All the numerical data were presented as mean ± SEM (n=6) and analyzed by one-way ANOVA (Fisher; $0.01 < *P \leq 0.05$; $**P \leq 0.01$; $***P \leq 0.001$).

Nature Chemical Biology: doi:10.1038/nchembio.2297

a

Group description	Median TTE (day)	TGD (day)	%TGD
DCL-AAM+DBCO-VC-Dox	60.0	23.1	62.6
DBCO-VC-Dox	47.6	10.7	29.0
DCL-AAM	38.0	1.1	3.0
PBS	36.9	--	--

c

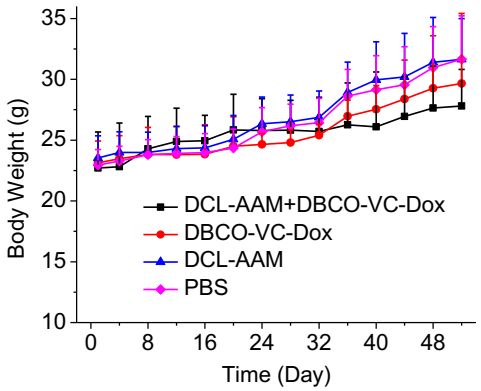

b

Group A	Group B	Day						
		16	20	24	28	32	36	40
DCL-AAM+DBCO-VC-Dox	PBS	*	**	**	**	**	**	***
DBCO-VC-Dox	PBS	n.s.	n.s.	n.s.	n.s.	n.s.	n.s.	*
DCL-AAM	PBS	n.s.	n.s.	n.s.	n.s.	n.s.	n.s.	n.s.
DCL-AAM+DBCO-VC-Dox	DBCO-VC-Dox	n.s.	n.s.	*	*	*	**	**
DCL-AAM+DBCO-VC-Dox	DCL-AAM	*	*	**	**	**	**	***

Supplementary Figure 16. DCL-AAM mediated tumor labeling significantly improved long-term antitumor efficacy of DBCO-VC-Dox against subcutaneous MDA-MB-231 tumors in athymic nude mice. MDA-MB-231 tumors were established in 6 week-old female athymic nude mice by subcutaneous injection of MDA-MB-231 cells into both flanks. When the tumors reached ~50 mm^3, mice were randomly divided into 4 groups (group 1: DCL-AAM+DBCO-VC-Dox; group 2: DBCO-VC-Dox; group 3: DCL-AAM; group 4: PBS; n = 5). DCL-AAM was i.v. injected on Day 0, 1, and 2. Subsequently DBCO-VC-Dox was i.v. injected on Day 3, 7, and 11. (a) Survival analysis of mice from different groups. TTE: time to end point. TGD: tumor growth delay; TGD = TTE (treated group)—TTE (PBS group). %TGD = 100% × TGD/TTE (PBS group). (b) Statistical analyses of the tumor volume by one-way ANOVA and Fisher's LSD test ($0.01 < *P \leq 0.05$; $**P \leq 0.01$; $***P \leq 0.001$). (c) Body weight of mice from different groups over the course of the efficacy study. Curves were truncated when three or more mice were dead or sacrificed.

Nature Chemical Biology: doi:10.1038/nchembio.2297

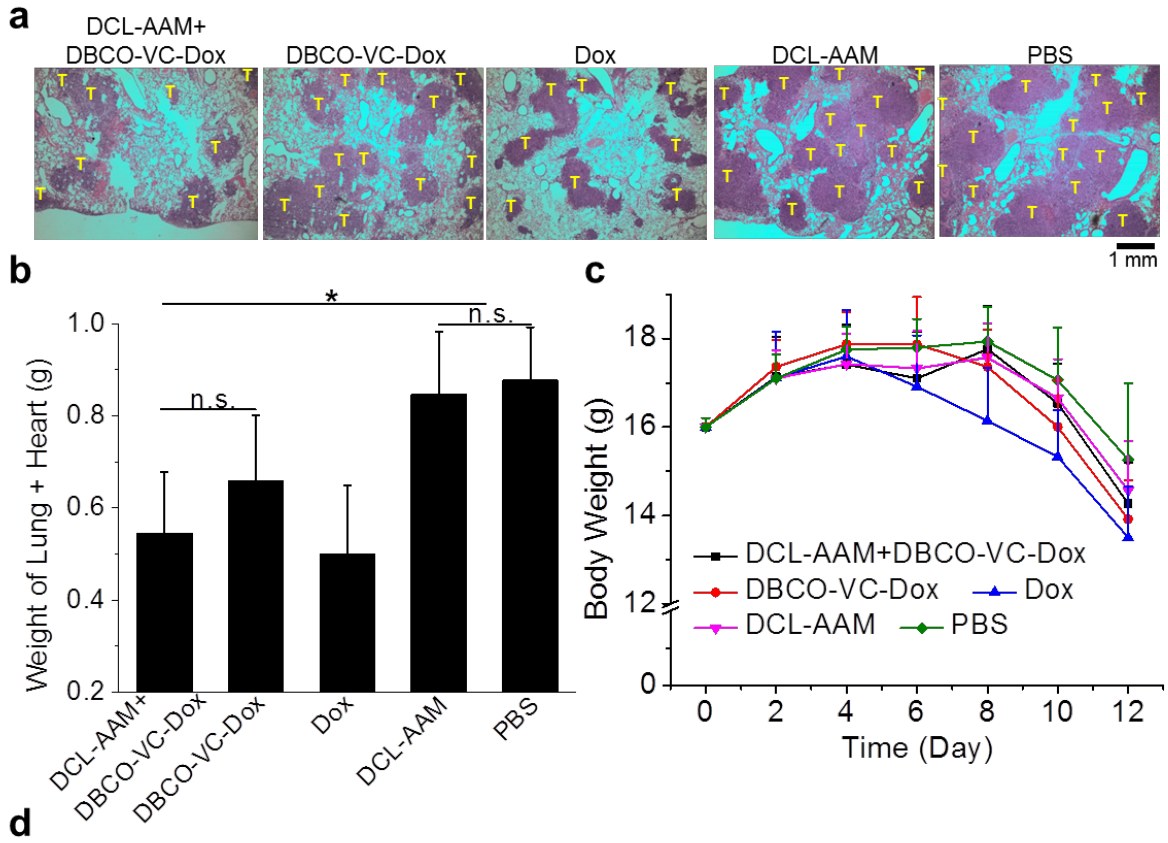

d

Acute toxicity		Dox[1]	DCL-AAM+DBCO-VC-Dox[2]	PBS
Bone marrow: Decreased cellularity		+/+++ (3/7)	-	-
Spleen	Decreased hematopoiesis	+++ (8/8)	-	-
	Decreased granulopoiesis	+++ (8/8)	-	-
	Lymphoid depletion	+ (8/8)	-	-

Supplementary Figure 17. DCL-AAM mediated cancer labeling significantly improved anticancer efficacy of DBCO-VC-Dox against 4T1 lung metastases in BALB/c mice. Luciferase-engineered 4T1 cells were i.v. injected into BALB/c mice on Day 0, and mice were randomly divided into 5 groups (group 1: DCL-AAM+DBCO-VC-Dox; group 2: DBCO-VC-Dox; group 3: Dox; group 4: DCL-AAM; group 5: PBS; n = 7-8). DCL-AAM (60 mg/kg) was i.v. injected once daily for three days (Day 1, 2, and 3). DBCO-VC-Dox (12 mg/kg in Dox equivalent) or Dox (7.5 mg/kg, maximum tolerated dose) was i.v. injected on Day 4, 8, and 12. (a) Representative images of H&E stained lung tissues of mice from different groups. T indicates tumor. Scale bar: 1 mm. (b) Weight of lung plus heart of mice from different groups (n=7-8). Statistical analyses were conducted by one-way ANOVA (Fisher; $0.01 < *P \leq 0.05$; $**P \leq 0.01$; $***P \leq 0.001$). (c) Body weight of BALB/c mice from different groups over the course of efficacy study. (d) Toxicity evaluation of Dox and DCL-AAM+DBCO-VC-Dox in BALB/c mice. [1]22.5 mg/kg Dox; [2]36.0 mg/kg Dox; + (mild); +++ (marked); - (negative).

Nature Chemical Biology: doi:10.1038/nchembio.2297

SUPPLEMENTARY NOTES

Selective In Vivo Metabolic Cell Labeling Mediated Cancer Targeting

Hua Wang[b,*], Ruibo Wang[b,*], Kaimin Cai[b,*], Hua He[a], Yang Liu[b], Jonathan Yen[c], Zhiyu Wang[b], Ming Xu[b], Yiwen Sun[b], Xin Zhou[d], Qian Yin[b], Li Tang[b], Iwona T. Dobrucki[e], Lawrence W. Dobrucki[c], Eric J. Chaney[f], Stephen A. Boppart[c,f,g,h], Timothy M. Fan[i,1], Stéphane Lezmi[j,1], Xuesi Chen,[p,1] Lichen Yin[a,1], Jianjun Cheng[a,b,c,k,l,m,n,o,1]

[a]Jiangsu Key Laboratory for Carbon-Based Functional Materials & Devices, Institute of Functional Nano & Soft Materials (FUNSOM), Soochow University, Suzhou 215123, Jiangsu, China.
[b]Department of Materials Science and Engineering, [c]Department of Bioengineering, [e]Molecular Imaging Laboratory, Beckman Institute for Advanced Science and Technology, [f]Biophotonics Imaging Laboratory, Beckman Institute for Advanced Science and Technology, [g]Department of Electrical and Computer Engineering, [h]Department of Internal Medicine, [i]Department of Veterinary Clinical Medicine, [j]Department of Pathobiology at College of Veterinary Medicine, [k]Department of Chemistry, [l]Beckman Institute for Advanced Science and Technology, [m]Micro and Nanotechnology Laboratory, [n]Institute of Genomic Biology, [o]Materials Research Laboratory, University of Illinois at Urbana–Champaign, Urbana, IL, 61801, USA.
[d]Department of Chemistry, University of Science and Technology of China, Hefei, Anhui 230026, China.
[p]Key Laboratory of Polymer Ecomaterials, Changchun Institute of Applied Chemistry, Changchun 130022, People's Republic of China

*These authors contributed equally to this work.

[1]To whom correspondence may be addressed. Email: jianjunc@illinois.edu; lcyin@suda.edu.cn; xschen@ciac.ac.cn; slezmi@illinois.edu; t-fan@illinois.edu.

Nature Chemical Biology: doi:10.1038/nchembio.2297

Table of Contents

Nature Chemical Biology: doi:10.1038/nchembio.2297

Supplementary Scheme 1. Synthetic route of Ac_4ManAz, $Ac_3ManAzEt$, and $Ac_3ManAzNB$

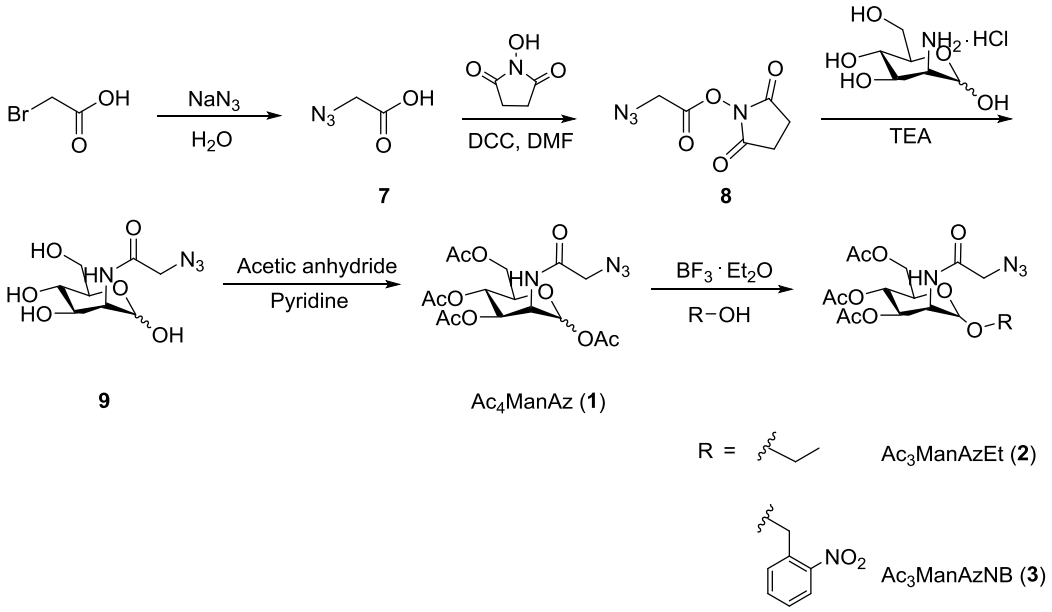

Synthesis of 2-azidoacetic acid (7). Bromoacetic acid (20 mmol) and sodium azide (40 mmol) were dissolved in deionized water and stirred at room temperature for 24 h. The resulting solution was adjusted to pH = 1 using hydrogen chloride solution, and then extracted with diethyl ether for three times. The organic phase was collected, dried over anhydrous sodium sulfate, and concentrated to yield 2-azidoacetic acid as colorless oil.

Synthesis of *N*-(2-azidoacetyl) succinimide (8). *N*,*N*′-Dicyclohexylcarbodiimide (DCC, 10 mmol) and **7** (10 mmol) were dissolved in anhydrous DMF, followed by the addition of *N*-hydroxysuccinimide (NHS, 10 mmol). The mixture was stirred at room temperature for 24 h. After filtrating off the precipitate, the solvent was removed to yield a yellow solid. The crude product was recrystallized from DCM/hexane to obtain a white solid. ^{1}H NMR ($CDCl_3$, 500 MHz): δ 4.25 (s, 2H, N_3CH_2), 2.88 (s, 4H, CH_2CH_2). ^{13}C NMR ($CDCl_3$, 500 MHz): 168.7, 164.4, 48.2, 25.8. ESI MS (*m/z*): calculated for $C_6H_7N_4O_4$ $[M+H]^+$ 199.0, found 199.0.

Synthesis of Ac_4ManAz (1). D-Mannosamine hydrochloride (2.5 mmol) and triethylamine (2.5 mmol) were dissolved in methanol, followed by the addition of **8** (2.75 mmol). The mixture was stirred at room temperature for 24 h. Solvent was removed under reduced pressure and the residue was re-dissolved in pyridine. Acetic anhydride was added and the reaction mixture was

Nature Chemical Biology: doi:10.1038/nchembio.2297

stirred at room temperature for another 24 h. After removal of the solvent, the crude product was purified by silica gel column chromatography using ethyl acetate/hexane (1/1, v/v) as the eluent to yield a white solid (1/1 α/β isomers). ^{1}H NMR ($CDCl_3$, 500 MHz): δ (ppm) 6.66&6.60 (d, *J*= 9.0 Hz, 1H, C(O)N*H*CH), 6.04&6.04 (d, 1H, *J*=1.9 Hz, NHCHC*H*O), 5.32-5.35&5.04-5.07 (dd, *J*=10.2, 4.2 Hz, 1H, CH_2CHC*H*CH), 5.22&5.16 (t, *J*=9.9 Hz, 1H, CH_2CHCHC*H*), 4.60-4.63&4.71-4.74 (m, 1H, NHC*H*CHO), 4.10-4.27 (m, 2H, C*H*$_2$CHCHCH), 4.07 (m, 2H, C(O)C*H*$_2$$N_3$), 3.80-4.04 (m, 1H, CH_2C*H*CHCH), 2.00-2.18 (s, 12H, C*H*$_3$C(O)). ^{13}C NMR ($CDCl_3$, 500 MHz): δ (ppm) 170.7, 170.4, 170.3, 169.8, 168.6, 168.3, 167.5, 166.9, 91.5, 90.5, 73.6, 71.7, 70.5, 69.1, 65.3, 65.1, 62.0, 61.9, 52.8, 52.6, 49.9, 49.5, 21.1, 21.0, 21.0, 20.9, 20.9, 20.9, 20.8. ESI MS (*m/z*): calculated for $C_{16}H_{22}N_4O_{10}Na$ $[M+Na]^+$ 453.1, found 453.1.

Synthesis of Ac$_3$ManAzEt (2) and Ac$_3$ManAzNB (3). Ac_4ManAz (0.1 mmol, see Supplementary Section 'Experimental') and ethanol or 2-nitrobenzylalcohol (0.3 mmol) were dissolved in dry dichloromethane. Boron trifluoride etherate (0.5 mmol) was added. The mixture was stirred overnight and then washed with saturated sodium bicarbonate solution and water. The organic phase was collected and concentrated to yield yellow oil. The crude product was purified by silica gel column chromatography using ethyl acetate/hexane (1/1, v/v) as the eluent.

Ac$_3$ManAzEt (2): ^{1}H NMR ($CDCl_3$, 500 MHz): δ (ppm) 6.52 (d, *J* = 9.1 Hz, 1H, C(O)N*H*CH), 5.35 (dd, *J* = 10.2, 4.2 Hz, 1H, CH_2CHC*H*CH), 5.13 (t, *J* = 10.1 Hz, 1H, CH_2CHCHC*H*), 4.77 (d, *J* = 1.7 Hz, 1H, NHCHC*H*O), 4.58 (ddd, *J* = 9.3, 4.3, 1.7 Hz, 1H, NHC*H*CHO), 4.21-4.26 (dd, *J* = 12.3, 4.5 Hz, 1H, C*H*$_2$CHCHCH), 4.11-4.15 (dd, *J* = 12.3, 2.4 Hz, 1H, C*H*$_2$CHCHCH), 4.05 (m, 2H, C(O)C*H*$_2$$N_3$), 3.99 (m, 1H, CH_2C*H*CHCH), 3.54&3.73 (dq, *J* = 9.5, 7.2 Hz, 2H, CH_3C*H*$_2$O), 1.98-2.12 (s, 9H, C*H*$_3$C(O)), 1.25 (t, 3H, C*H*$_3$$CH_2$O). ^{13}C NMR ($CDCl_3$, 500 MHz): δ (ppm) 170.8, 170.3, 170.0, 166.9, 98.7, 69.5, 68.3, 66.1, 64.3, 62.4, 52.7, 51.1, 21.0, 20.9, 20.9, 15.1. HR ESI MS (*m/z*): calculated for $C_{16}H_{23}N_4O_9$ $[M-H]^-$ 415.1465, found 415.1460.

Ac$_3$ManAzNB (3): ^{1}H NMR ($CDCl_3$, 500 MHz): δ (ppm) 8.12 (d, *J* = 8.2 Hz, 1H, Ph, CHCHCHC*H*NO_2), 7.79 (d, *J* = 7.5 Hz, 1H, Ph, C*H*CHCHCHNO_2), 7.72 (t, *J* = 7.5 Hz, 1H, Ph, CHC*H*CHCHNO_2), 7.50 (t, *J* = 8.4, 7.5 Hz, 1H, Ph, CHCHC*H*CHNO_2), 6.57 (d, *J* = 8.9 Hz, 1H, C(O)N*H*CH), 5.41 (dd, *J* = 10.1, 4.2 Hz, 1H, CH_2CHC*H*CH), 5.14-5.20 (m, 2H, C(O)NHCHC*H*O, CH_2CHCHC*H*), 4.94 (dd, *J* = 8.4, 6.6 Hz, 2H, OC*H*$_2$Ph), 4.76 (ddd, *J* = 9.3, 4.4, 1.8 Hz, 1H, C(O)NHC*H*CHO), 4.22-4.28 (dd, *J* = 12.4, 4.9 Hz, 1H, C*H*$_2$CHCHCH), 4.11-

Nature Chemical Biology: doi:10.1038/nchembio.2297

4.15 (dd, *J* = 12.9, 3.1 Hz, 1H, C*H*$_2$CHCHCH), 4.06 (m, 2H, C(O)C*H*$_2$N$_3$), 4.02 (m, 1H, CH$_2$C*H*CHCH), 2.01-2.13 (s, 9H, C*H*$_3$C(O)). ^{13}C NMR (CDCl$_3$, 500 MHz): δ (ppm) 170.8, 170.0, 167.0, 134.4, 128.8, 128.7, 125.2, 98.7, 69.5, 69.0, 66.6, 65.8, 62.3, 52.7, 50.4, 21.0, 20.9, 20.8. HR ESI MS (*m/z*): calculated for $C_{21}H_{26}N_5O_{11}$ $[M+H]^+$ 524.1629, found 524.1635.

Supplementary Scheme 2. Synthetic route of HDAC/CTSL responsive DCL-AAM

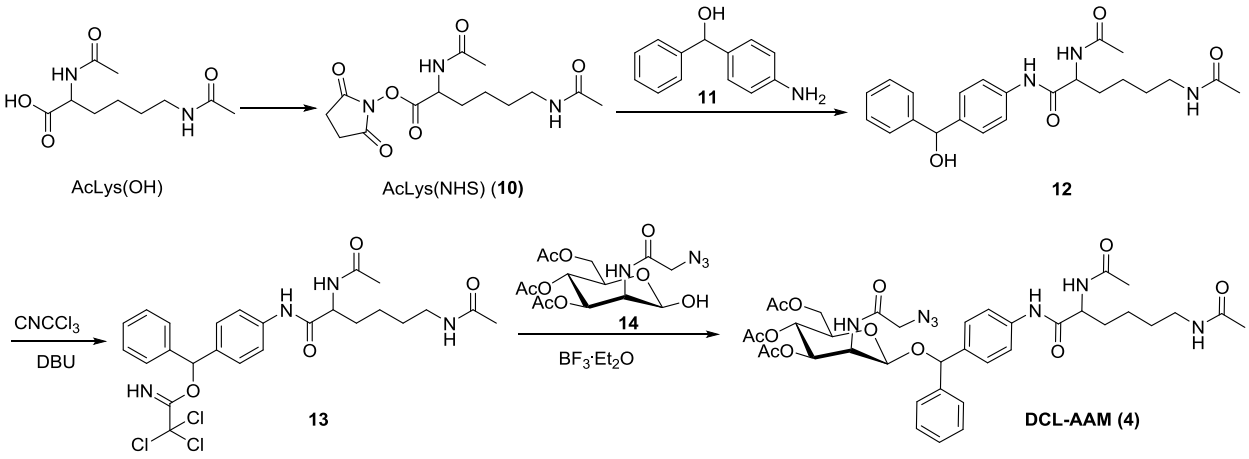

Synthesis of AcLys(NHS) (10). AcLys(OH) (2.0 mmol) and triethylamine (2.1 mmol) was dissolved in anhydrous DMF, followed by the addition of DCC (2.1 mmol) and NHS (2.1 mmol). The reaction mixture was stirred at room temperature for 24 h. The precipitate was filtered off, and the solvent was removed under reduced pressure. The crude product was directly used without further purification.

Synthesis of (4-aminophenyl)(phenyl)methanol (11). 4-Aminobenzophenone (5.0 mmol) was dissolved in dry methanol, followed by addition of sodium borohydride (10.0 mmol). The mixture was stirred at room temperature for 24 h. After removal of the solvent, the crude product was purified by silica gel column chromatography using hexane/ethyl acetate (6/1 to 3/1) as the eluent. Compound **11** was obtained as a light yellow solid. ^{1}H NMR (CDCl$_3$, 500 MHz): δ (ppm) 7.38 (d, 2H, Ph), 7.32 (t, 2H, Ph), 7.25 (t, 1H, Ph), 7.14 (d, 2H, Ph), 6.63 (d, 2H, Ph), 5.75 (s, 1H, C*H*(OH)), 3.65 (s, 1H, (CH(O*H*)), 3.45 (s, 2H, N*H*$_2$). ^{13}C NMR (CDCl$_3$, 500 MHz): δ (ppm) 146.1, 144.4, 134.4, 128.6, 128.2, 127.5, 126.6, 115.3, 76.2. ESI MS (*m/z*): calculated for $C_{13}H_{14}NO$ $[M+H]^+$ 200.1, found 200.1.

Nature Chemical Biology: doi:10.1038/nchembio.2297

Synthesis of AcLys(DPM) (12). AcLys(NHS) (1.2 mmol) and compound **11** (1.2 mmol) were dissolved in anhydrous DMF, followed by the addition of triethylamine (1.2 mmol). The mixture was stirred at 40^{o}C for 24 h. After removal of the solvent, the crude product was purified by silica gel column chromatography using ethyl acetate to ethyl acetate/methanol (20/1, v/v) as the eluent to yield a light yellow solid. ^{1}H NMR (CD_3OD, 500 MHz): δ (ppm) 7.50 (d, 2H, Ph), 7.34 (d, 2H, Ph), 7.29 (m, 4H, Ph), 7.21 (t, 1H, Ph), 5.74 (s, 1H, C*H*(OH)), 4.39 (m, 1H, C*H*$CH_2CH_2CH_2CH_2NHC(O)CH_3$), 3.15 (t, 2H, $CHCH_2CH_2CH_2CH_2NHC(O)CH_3$), 2.00 (s, 3H, $CHCH_2CH_2CH_2CH_2NHC(O)CH_3$), 1.89 (s, 3H, $CHNHC(O)CH_3$), 1.83&1.72 (m, 2H, $CHCH_2CH_2CH_2CH_2NHC(O)CH_3$), 1.53 (m, 2H, $CHCH_2CH_2CH_2CH_2CH_2NHC(O)CH_3$), 1.41 (m, 2H, $CHCH_2CH_2CH_2CH_2NHC(O)CH_3$). ^{13}C NMR ($CD_3OD$, 500 MHz): 172.2, 172.0, 171.7, 144.7, 140.9, 137.3, 128.1, 127.0, 126.5, 120.1, 75.3, 54.4, 38.9, 31.7, 28.9, 23.1, 21.4, 21.2. ESI MS (*m/z*): calculated for $C_{23}H_{29}N_3O_4Na$ $[M+Na]^+$ 434.2, found 434.2.

Synthesis of **AcLys(DPM-CNCCl$_3$) (13)**. Compound **12** (0.5 mmol) and $CNCCl_3$ (5.0 mmol) were dissolved in anhydrous THF, followed by the addition of 1,8-diazabicycloundec-7-ene (DBU, 0.5 mmol). The reaction mixture was stirred at room temperature for 4 h. After removal of the solvent, the crude product was purified by silica gel column chromatography to yield a white solid. ^{1}H NMR (CD_3OD, 500 MHz) δ (ppm) 7.99 (m, 1H), 7.53 (d, *J* = 8.4 Hz, 2H), 7.38–7.19 (m, 7H), 5.27 (s, 1H), 4.43 (m, 1H), 3.73 (m, 1H), 3.17 (m, 2H), 2.02 (s, 3H), 1.91 (s, 3H), 1.84&1.73 (m, 2H), 1.55 (m, 2H), 1.44 (m, 2H). ^{13}C NMR (CD_3OD, 500 MHz): 208.42, 172.2, 172.1, 171.7, 142.4, 138.5, 137.6, 128.2, 127.3, 126.8, 120.2, 101.8, 85.0, 64.4, 54.3, 39.1, 31.7, 28.9, 23.1, 21.4, 21.3.

Synthesis of Ac$_3$ManAzOH (14). Ac_4ManAz (0.5 mmol) and ammonium carbonate (0.75 mmol) were dissolved in THF/methanol (2/1, v/v) and stirred at room temperature. After 12 h, the solvent was removed and the crude product was purified by silica gel column chromatography to yield a white solid. ^{1}H NMR ($CDCl_3$, 500 MHz): δ (ppm) 6.56 (d, *J* = 9.2 Hz, 1H), 5.44 (dd, *J* = 10.1, 4.2 Hz, 1H), 5.22 (s, 1H), 5.18 (t, 1H), 4.63 (ddd, *J* = 9.2, 4.2, 1.8 Hz, 1H), 4.31 – 4.01 (m, 5H), 3.74 (m, 1H), 2.14&2.08&2.05 (s, 9H). ^{13}C NMR ($CDCl_3$, 500 MHz): δ (ppm) 171.0, 170.4, 170.1, 167.1, 93.4, 69.2, 68.4, 66.0, 62.5, 52.7, 50.9, 21.1, 21.0, 20.9.

Nature Chemical Biology: doi:10.1038/nchembio.2297

Synthesis of DCL-AAM (4). Ac_3ManAzOH (0.2 mmol) and AcLys(DPM-$CNCCl_3$) (0.22 mmol) were dissolved in anhydrous acetonitrile, followed by the addition of boron trifluoride etherate (2.0 mmol). The mixture was stirred at 0°C for 1 h. After removal of the solvent, the crude product was purified by silica gel column chromatography and HPLC to yield a white solid. ^{1}H NMR ($CDCl_3$, 500 MHz): δ (ppm) 7.55 (m, 2H, Ph), 7.35-7.28 (m, 7H, Ph), 6.73 (m, 1H, $CH_3C(O)NHCH$), 6.50 (m, 1H, $CH_2C(O)NHCH$), 5.95 (m, 1H, $CH_3C(O)NHCH_2$), 5.65 (s, 1H, PhC*H*), 5.43 (ddd, *J* = 10.1, 8.3, 4.2 Hz, 1H, $CH_2CHCHCH$), 5.17 (td, *J* = 10.2, 3.2 Hz, 1H, $CH_2CHCHCH$), 4.75-4.80 (m, 1H, NHCHC*H*O), 4.68 (m, 1H, NHC*H*CHO), 4.55 (q, *J* = 7.3 Hz, 1H, $CHCH_2CH_2CH_2CH_2NHC(O)CH_3$), 4.18&4.05 (m, 2H, $CH_2CHCHCH$), 4.02 (m, 2H, $COCH_2N_3$), 3.94 (m, 1H, $CH_2CHCHCH$), 3.22 (m, 2H, $CHCH_2CH_2CH_2CH_2NHC(O)CH_3$), 2.12&2.06&2.03&1.99&1.96 (15H, $CH_3C(O)O$), 1.93&1.74 (m, 2H, $CHCH_2CH_2CH_2CH_2NHC(O)CH_3$), 1.51 (m, 2H, $CHCH_2CH_2CH_2CH_2NHC(O)CH_3$), 1.38 (m, 2H, $CHCH_2CH_2CH_2CH_2NHC(O)CH_3$). ^{13}C NMR ($CDCl_3$, 500 MHz): δ(ppm) 171.5, 171.2, 170.7, 170.4, 170.0, 170.0, 166.8, 141.2, 137.8, 137.2, 135.6, 129.1, 128.8, 128.5, 127.5, 126.7, 120.2, 80.0, 77.5, 77.5, 77.3, 77.2, 77.0, 69.9, 69.0, 65.8, 62.3, 53.9, 52.7, 50.5, 38.8, 31.3, 29.1, 23.4, 22.5, 21.1, 20.9. HR ESI MS (*m/z*): calculated for $C_{37}H_{48}N_7O_{12}$ $[M+H]^+$ 782.3361, found 782.3354.

Supplementary Scheme 3. Synthetic route of HDAC/CTSL fluorescent reporter (Naph-Lys)

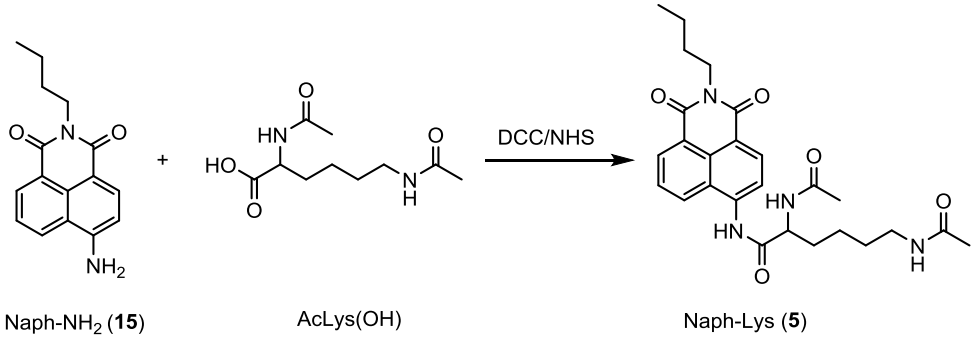

Nature Chemical Biology: doi:10.1038/nchembio.2297

Syntheis of Naph-NH_2 (15). 4-Amino-1,8-naphthalic anhydride (10 mmol) was dissolved in ethanol (100 mL) under nitrogen atmosphere and brought to reflux. 1-butylamine (15 mmol) was then added and the mixture was further refluxed for 8 h. After cooling down, the solvent was removed under reduced pressure, and the crude product was purified by silica gel column chromatography using DCM/ethyl acetate (2/1, v/v) as the eluent. ^{1}H NMR ($CDCl_3$, 500 MHz): δ (ppm) 8.60 (d, 1H, C(O)CC*H*CHCH), 8.42 (d, 1H, C(O)CCHCHC*H*), 8.10 (d, 1H C(O)CCHC*H*CH), 7.66 (t, 1H, C(O)CC*H*CH), 6.89 (d, 1H, C(O)CCHC*H*), 4.94 (s, 2H, NH_2), 4.18 (t, 2H, C$H_2$$CH_2CH_2CH_3$), 1.71 (m, 2H, CH_2C$H_2$$CH_2CH_3$), 1.45 (m, 2H, CH_2CH_2C$H_2$$CH_3$), 0.97 (s, 3H, $CH_2CH_2CH_2$CH_3). ESI MS (*m/z*): calculated for $C_{16}H_{17}N_2O_4$ $[M+H]^+$ 269.1, found 269.1.

Synthesis of Naph-Lys (5). Naph-NH_2 (1.0 mmol) and AcLys(OH) (1.0 mmol) were dissolved in DMF, followed by the addition of DCC (1.1 mmol), NHS (1.1 mmol), and triethylamine (1.0 mmol). The mixture was stirred at 45^{o}C for 48 h. After removal of precipitate and solvent, the crude product was purified by silica gel column chromatography using hexane/ethyl acetate as the eluent to yield a yellow solid. ^{1}H NMR (CD_3OD, 500 MHz): δ (ppm) 8.57 (dd, 1H, C(O)CC*H*CHCH), 8.52 (d, 1H C(O)CC*H*CH), 8.51 (dd, 1H, C(O)CCHCHC*H*), 8.12 (dd, 1H, C(O)CCHC*H*), 7.84 (dd, 1H, C(O)CCHC*H*CH), 4.62 (dd, 1H, C*H*$CH_2CH_2CH_2CH_2$), 4.14 (t, 2H, C$H_2$$CH_2CH_2CH_3$), 3.22 (t, 2H, $CHCH_2CH_2CH_2$CH_2), 2.06 (s, 3H, CH_3C(O)NHCH), 1.98 (m, 2H, CHC$H_2$$CH_2CH_2CH_2$), 1.92 (s, 3H, C$H_3$C(O)N$HCH_2$), 1.69 (m, 2H, CH_2C$H_2$$CH_2CH_3$), 1.60 (m, 2H, $CHCH_2CH_2$C$H_2$$CH_2$), 1.53 (m, 2H, $CHCH_2$C$H_2$$CH_2CH_2$), 1.43 (m, 2H, CH_2CH_2C$H_2$$CH_3$), 0.99 (m, 3H, $CH_2CH_2CH_2$CH_3). ESI MS (*m/z*): calculated for $C_{26}H_{33}N_4O_5$ $[M+H]^+$ 481.2, found 481.2.

Supplementary Scheme 4. Radiolabeling of DCL-AAM

Nature Chemical Biology: doi:10.1038/nchembio.2297

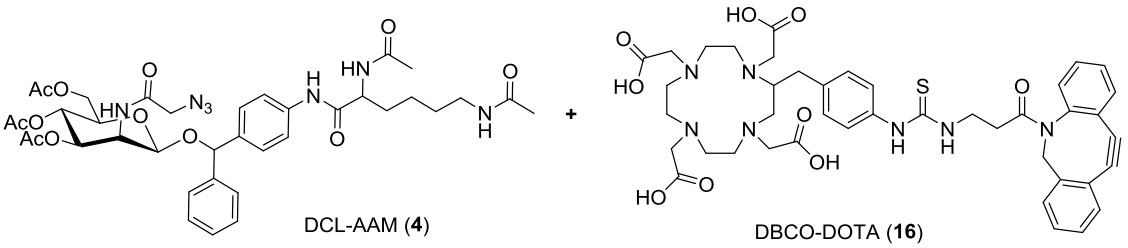

DCL-AAM (**4**)

DBCO-DOTA (**16**)

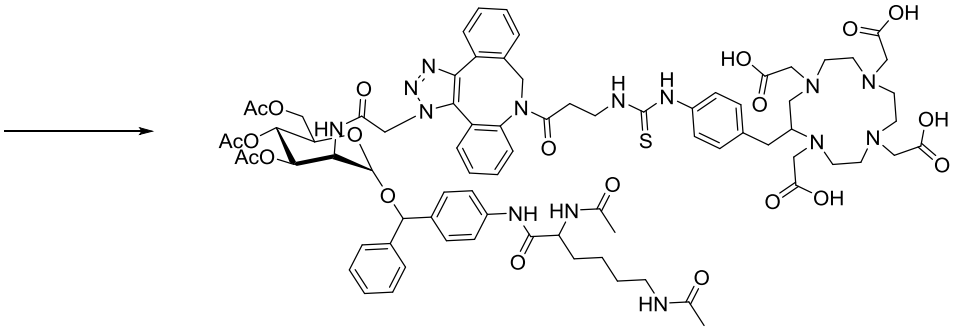

DCL-AAM-DOTA (**17**)

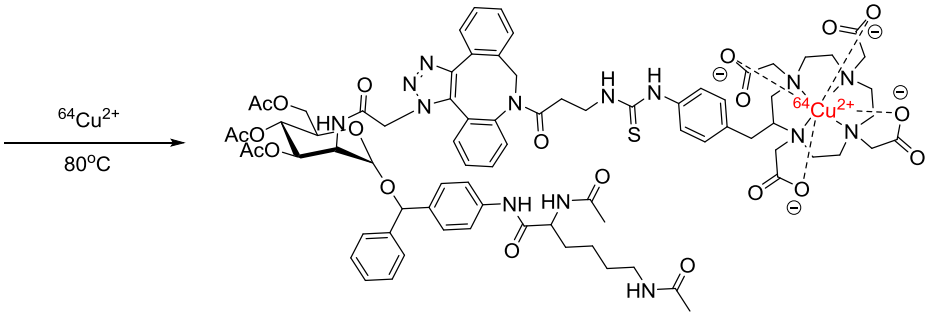

DCL-AAM-DOTA-^{64}Cu (**18**)

Synthesis of DBCO-DOTA (16). *P*-SCN-Bn-DOTA (0.05 mmol) and DBCO-amine (0.05 mmol) were suspended in anhydrous DMF (1 mL). Triethylamine (0.2 mmol) was added and the mixture was stirred at 40°C for 12 h. The solvent was removed under reduced pressure and the product was used without further purification. ESI MS (*m/z*): calculated for $C_{42}H_{50}N_7O_9S$ $[M+H]^+$ 828.3, found 828.3.

Synthesis of DCL-AAM-DOTA (17). DBCO-DOTA (0.01 mmol) and DCL-AAM (0.01 mmol) were dissolved in methanol. The mixture was stirred at room temperature for 1 h, at which time point HPLC showed complete consumption of the starting materials. The product was lyophilized and used directly without further purification.

Nature Chemical Biology: doi:10.1038/nchembio.2297

Synthesis of ^{64}Cu-labeled DCL-AAM (18). The ^{64}Cu chloride (400 μCi, 0.1 ng of ^{64}Cu) in NH_4OAc buffer solution (0.1 M, pH = 5.5, 1 mL) was mixed with DCL-AAM-DOTA (2 mg) in PBS. The mixture was vigorously stirred at 80°C for 1 h, at which time point HPLC showed complete consumption of free ^{64}Cu. The product solution was directly used without further purification.

Supplementary Scheme 5. Synthetic route of DBCO-VC-Dox

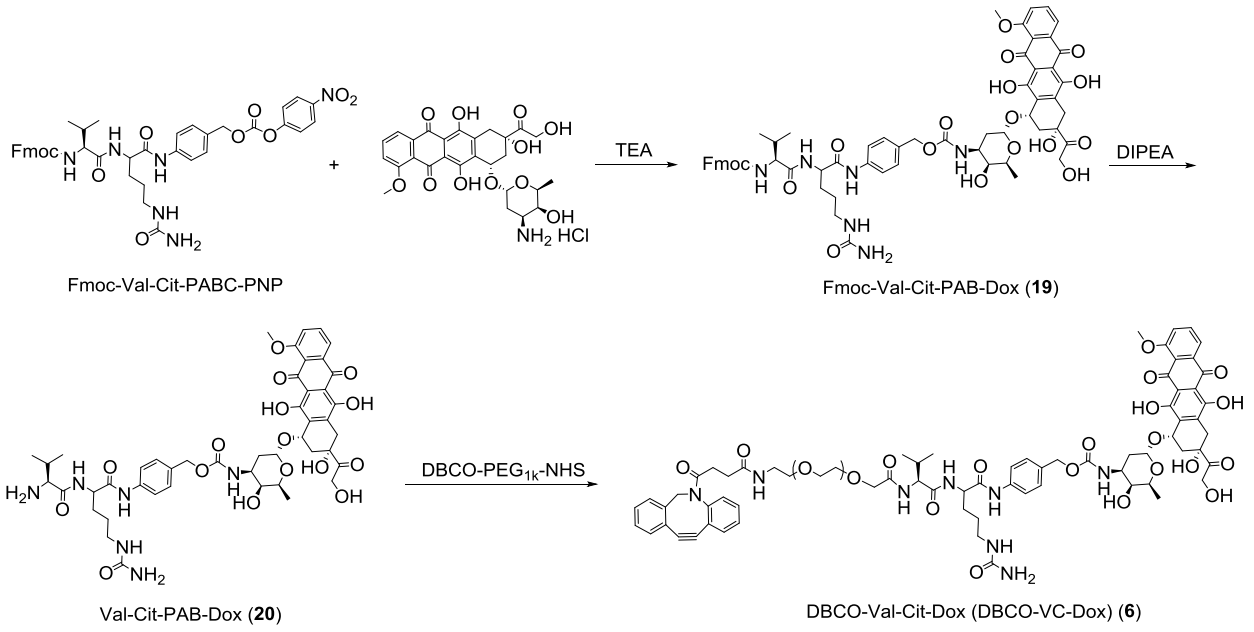

Synthesis of DBCO-PEG$_{1k}$-NHS. DBCO-NHS (0.11 mmol) and NH_2-PEG$_{1k}$-COOH (0.10 mmol) were dissolved in anhydrous DMF, followed by the addition of triethylamine (0.11 mmol). The mixture was stirred at 45°C for 24 h. DCC (0.12 mmol) and NHS (0.12 mmol) in DMF were added. The reaction mixture was further stirred at 45°C for 24 h. The precipitate was filtered off and the filtrate was ultracentrifuged (repeated twice) with a cut-off molecular weight of 1k. The residual solution was diluted with DCM, collected, and concentrated to yield a light yellow solid (70% yield).

Synthesis of DBCO-VC-Dox (6). Doxorubicin hydrochloride (0.05 mmol), Fmoc-Val-Cit-PAB-PNP (0.05 mmol) and triethylamine (0.06 mmol) were dissolved in dimethylformamide and stirred at 40°C for 12 h, at which point diisopropylethylamine (100 μL) was added. After 12 h, DBCO-PEG$_{1k}$-NHS (0.05 mmol, see Supplementary Section 'Experimental') was added and the

Nature Chemical Biology: doi:10.1038/nchembio.2297

mixture was stirred at 40^{o}C for another 24 h. The reaction solution was precipitated into diethyl ether to yield a red solid, which was purified by dialysis (1k cut-off molecular weight) for 48 h. MALDI MS (*m/z*) for DBCO-VC-Dox 1381.44+44.05*n, found 2262.4 (n=20), 2306.5 (n=21), 2350.5 (n=22), 2394.6 (n=23), 2438.6 (n=24), 2482.7 (n=25), 2526.7 (n=26), 2570.8 (n=27), 2658.9 (n=28).

Nature Chemical Biology: doi:10.1038/nchembio.2297